



Global miRNA, lncRNA, and mRNA Transcriptome Profiling of Endometrial Epithelial Cells Reveals Genes Related to Porcine Reproductive Failure Caused by Porcine Reproductive and Respiratory Syndrome Virus

OPEN ACCESS

Edited by:

Falko Steinbach,
University of Surrey, United Kingdom

Reviewed by:

Xiaobo Zhang,
Zhejiang University, China
Anastasia N. Vlasova,
The Ohio State University,
United States

*Correspondence:

Feng Su
suf@sdau.edu.cn
Yunliang Jiang
yjliang723@aliyun.com

†These authors have contributed
equally to this work

Specialty section:

This article was submitted to
Comparative Immunology,
a section of the journal
Frontiers in Immunology

Received: 19 November 2018

Accepted: 13 May 2019

Published: 04 June 2019

Citation:

Zhang K, Ge L, Dong S, Liu Y,
Wang D, Zhou C, Ma C, Wang Y, Su F
and Jiang Y (2019) Global miRNA,
lncRNA, and mRNA Transcriptome
Profiling of Endometrial Epithelial Cells
Reveals Genes Related to Porcine
Reproductive Failure Caused by
Porcine Reproductive and Respiratory
Syndrome Virus.
Front. Immunol. 10:1221.
doi: 10.3389/fimmu.2019.01221

**Kang Zhang^{1†}, Lijiang Ge^{1†}, Shasha Dong^{2†}, Ying Liu¹, Dong Wang¹, Chunyan Zhou¹,
Cai Ma¹, Yanchao Wang¹, Feng Su^{1*} and Yunliang Jiang^{1*}**

¹ Shandong Provincial Key Laboratory of Animal Biotechnology and Disease Control and Prevention, College of Animal Science and Technology, Shandong Agricultural University, Taian, China, ² Department of Cardiology, Shandong First Medical University and Shandong Academy of Medical Science, Taian, China

Porcine reproductive and respiratory syndrome virus (PRRSV) can cause respiratory disease and reproductive failure in pregnant pigs. Previous transcriptome analyses in susceptible cells have mainly concentrated on pulmonary alveolar macrophages (PAM) and Marc-145 cells, and on the respiratory system. Some studies reported that apoptosis of placental cells and pig endometrial epithelial cells (PECs) is an obvious sign linked to reproductive failure in pregnant sows, but the mechanism is still unknown. In this study, Sn-positive PECs were isolated and apoptosis rates were assessed by flow cytometry. PRRSV-infected PECs exhibited apoptosis, indicative of their susceptibility to PRRSV. Subsequently, the whole transcriptome was compared between mock- and PRRSV-infected PECs and 54 differentially expressed microRNAs (DEmiRNAs), 104 differentially expressed genes (DEGs), 22 differentially expressed lncRNAs (DElncRNAs), and 109 isoforms were obtained, which were mainly enriched in apoptosis, necroptosis, and p53 signal pathways. Integration analysis of DEmiRNA and DEG profiles revealed two microRNAs (*ssc-miR-339-5p* and *ssc-miR-181d-5p*) and five genes (*SLA-DQB1*, *THBS1*, *SLC3A1*, *ZFP37*, and *LOC100517161*) participating in the apoptosis signal, of which *THBS1* and *SLC3A1* were mainly linked to the p53 pathway. Integration analysis of DEGs with DElncRNA profiles identified genes involved in apoptosis signal pathway are regulated by *LTCONS_00010766* and *LTCONS_00045988*. Pathway enrichment revealed that the phagosome and p53 pathways are the two main signals causing apoptosis of PECs, and functional analysis revealed a role of *miR-339-5p* in regulating apoptosis of PECs after PRRSV inoculation.

Keywords: PRRSV, PECs, lncRNA, mRNA, integrated analysis

INTRODUCTION

Porcine reproductive and respiratory syndrome (PRRS), an infectious viral disease, results in tremendous economic loss in the swine industry, through reproductive failure in breeding sows, and respiratory disorders in young and growing pigs (1). The porcine reproductive and respiratory syndrome virus (PRRSV) mainly causes reproductive failure in pregnant sows in the late period (2). Previous studies have reported that PRRSV exhibits infection permissiveness causing CD163⁺ and Sn⁺ lymphocyte apoptosis (3). The distribution of these positive cells explains the infectious attributes of PRRSV, which ultimately causes reproductive failure (3). Subsequently, in assays carried out by Feng and colleagues, CD163⁺ pig endometrial epithelial cells (PECs) were isolated and it was verified that PRRSV could replicate in these cells (4). A recent study showed that PRRSV could cause placental cell and PEC apoptosis and autophagy in the implantation site, leading to reproductive failure in the later phases of pregnancy (5).

Placental cell and PEC apoptosis have been recognized as obvious signs linked to reproductive failure in pregnant sows (6, 7). In a previous study, it was reported that PRRSV could cause apoptosis of Marc-145 cells through a mitochondria-mediated pathway (8). More recently, PRRSV was confirmed to lead not only to apoptosis, but also to autophagy of Marc-145 cells; in addition, cell apoptosis was proven to be the major reason for reduction of virus replication (9). In a study by Huo and colleagues, p53 protein was activated in PRRSV-infected Marc-145 cells and the activation of the JNK pathway induced cell apoptosis (10, 11). However, these studies mainly focused on Marc-145 cells and PAM cells, and no assays were reported to explain the mechanism underlying PRRSV-induced PEC apoptosis.

Cell apoptosis is a complicated process that is regulated by multiple factors. Expression of mRNA and miRNA in target cells in response to PRRSV has been investigated and differentially expressed mRNAs and differentially expressed miRNAs (DEmiRNAs) have been screened (12–17). However, the identified mRNAs and miRNAs were mainly related to PRRSV replication and organism immunity, and few were related to apoptosis caused by PRRSV. The lncRNA profile changes of PRRSV-infected PAM cells were investigated and a series of lncRNAs were screened and identified (12). Consistent with miRNA and mRNA studies, the identified lncRNAs were mainly involved in immune system. Some miRNAs were found to be involved in apoptosis and act as regulators of the mitochondrial apoptosis pathway (18–20). Some lncRNAs have been reported as negative regulators and taking part in the cell apoptosis pathway (20–22). However, the DEmiRNAs and differentially expressed lncRNAs (DELncRNAs) that participate in PRRSV-infected PECs are still unknown.

Abbreviations: DEG, differentially expressed gene; DELncRNA, differentially expressed lncRNA; DEmiRNA, differentially expressed miRNA; FC, fold change; FDR, false discovery rate; GO, gene ontology; miRNA, microRNA; PAM, pulmonary alveolar macrophages; PEC, pig endometrial epithelial cell; PRRSV, porcine reproductive and respiratory syndrome virus; ceRNA, competing endogenous RNAs.

TABLE 1 | Primers used in this study.

Genes	Strand	Sequence (5'-3')	Length	Annealing temperature (°C)
Loc100517161	F	AGGCTCACTGTCATTCAAG	290	60
	R	CCATAGTTTCAGGTTGC		
SLC3A1	F	GTGGCTTCTGTGCTTGCG	140	60
	R	CCGTTCCCGTCTTTGTGCG		
THBS1	F	CAATCCTTGCTTTGCTGGTG	264	59
	R	TTGTTGGCGGTGGCGTAT		
SLA-DQB1	F	CAGATAGAGGAAGGCACGACC	138	61
	R	GACTTTCACCTGGCTTGGATAG		
ZFP37	F	TGAGAAGTTATCCAACCGTAGC	391	60
	R	ATGGTCAGTGAGGGCGTGT		
GAPDH	F	TGGTGAAGTCCGGAGTGAAC	225	60
	R	GGAAGATGGTGATGGGATTTTC		
ssc-miR-181d-5p	F	CATTTCATTGTTGTCGGTGGGTT		60
ssc-miR-339-5p	F	GATTCCAGGAGCTCACGAAA		60
U6	F	CTCGCTTCGGCAGCACACA		60
	R	AACGCTTCACGAATTTGCGT		
miR-339-5p inhibitor		GUGAGCUCCUGGAGGACAGGGA		

In this study, we isolated Sn⁺ PECs and reported what is believed to be the first comprehensive and integrative analysis of the mRNAs, miRNAs, and lncRNAs underlying apoptosis in PRRSV-infected PECs. Changes in some mRNA and miRNA relating to the key genes of PRRSV-infected PECs were also characterized. Moreover, using these data, we have unveiled several candidate genes and signaling pathways related to apoptosis of PECs caused by PRRSV.

MATERIALS AND METHODS

Ethics Statement

All sows used in this study were housed in livestock housing and fed *ad libitum*. The sacrifice of sows was carried out with sodium barbital after anesthesia. All procedures involving animals were approved by the Animal Care and Use Committee of Shandong Agricultural University.

Cell Culture and Isolation

Sows of the Large White pig breed were used, which had not been vaccinated against PRRSV since birth. The sows were sacrificed at the age of 4 months. The uterus of each pig was removed and used for cell culture. The endometrium epithelial layer was isolated and cut into 1 mm³ cubes, then the cells were cultured in DMEM-F12 medium containing 10% fetal bovine serum (Gibco, Invitrogen, Carlsbad, CA, USA) and epidermal growth factor (10 ng/mL; Sigma, USA) using the tissue explant adherence method. After PEC clones had formed and expanded, Sn protein was used as a specificity marker for PEC identification. Briefly, the cells were fixed with polyformaldehyde for 24 h, and then the cells were incubated with Cytokeratin-18 (Beyotime, Jiangsu, China) and Sialoadhesin antibodies (ab94715; Abcom,

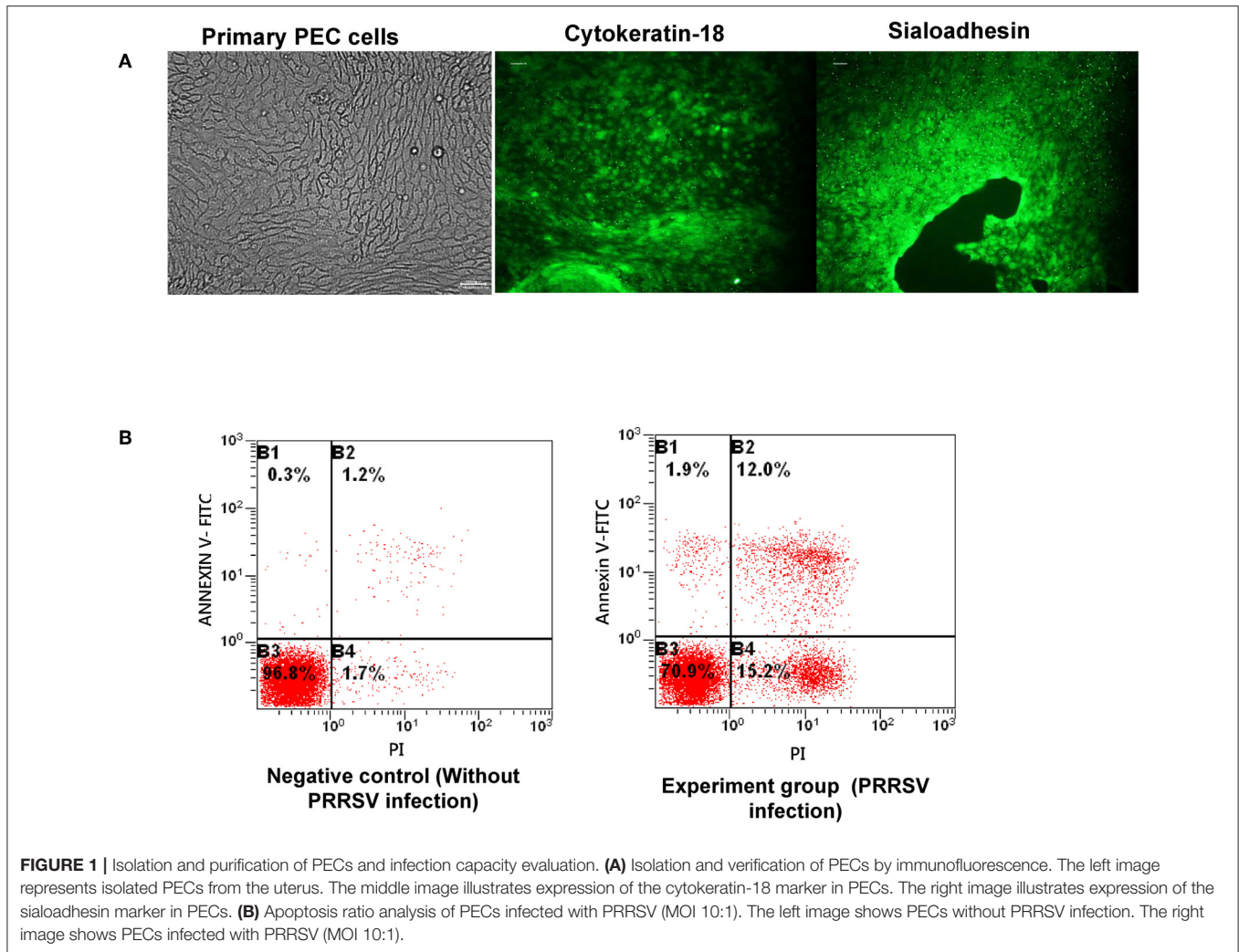


FIGURE 1 | Isolation and purification of PECs and infection capacity evaluation. **(A)** Isolation and verification of PECs by immunofluorescence. The left image represents isolated PECs from the uterus. The middle image illustrates expression of the cytokeratin-18 marker in PECs. The right image illustrates expression of the sialoadhesin marker in PECs. **(B)** Apoptosis ratio analysis of PECs infected with PRRSV (MOI 10:1). The left image shows PECs without PRRSV infection. The right image shows PECs infected with PRRSV (MOI 10:1).

Cambridge, USA) separately, after being incubated with blocking buffer (Beyotime, Jiangsu, China) for 4 h. The cells were then incubated with goat anti-rabbit antibody for 2 h, after being washed with washing buffer three times. The cells were then examined microscopically.

PRRSV Infection and Cell Apoptosis Analysis

PRRSV was kindly donated by Dr. Xiao of Shandong Agricultural University. PRRSV infection and titration were performed as described previously (23). Rates of PRRSV-induced cell apoptosis in PECs were determined by flow cytometry using the Annexin V-FITC Apoptosis Detection Kit (Beyotime), following the manufacturer's instructions. Briefly, PECs were incubated with PRRSV for 24 h, washed twice with ice-cold PBS, and then 5 μ L of annexin V-FITC and 1 μ L of PI (1 mg/mL) were applied to stain the cells. The stained cells were analyzed using a flow cytometer.

Sample Collection and Preparation

Isolated porcine endometrial cells were divided into two groups. One group was defined as the control group (without PRRSV

infection) and the other as the experiment group (infected with PRRSV, as mentioned above). All the samples were sent to Beijing Genomics Institute (BGI) for entire transcriptome sequencing. Each group consists of three technical replicate samples.

Total RNA Extraction

Total RNA was extracted using TRIzol reagent (Sigma) and treated with DNase to remove potential genomic DNA contamination, following the manufacturer's protocol. The quantity and purity of the total RNA were evaluated. RNA integrity was checked by microcapillary electrophoresis using an Agilent 2100 Bioanalyzer with an RNA 6000 Nanochip kit. The RNA was then divided into two aliquots that were used for library construction of either small RNA or RNA.

Preparation of the RNA-Seq Library

Total RNA was divided into two samples after preparation. In one sample, ribosomal RNA was removed by Epicenter Ribo-zero™ rRNA Removal Kit (Epicenter, Madison, WI, USA), and residual RNAs were cleaned by ethanol precipitation. The sequencing libraries were generated using rRNA-depleted RNA

TABLE 2 | Differential miRNA expression.

miRNA id	log2Ratio (Sample/control)	Up/down regulation	P-value	Q-value
novel_mir15	-1.944690794	DOWN	0	0
novel_mir35	-1.085608983	DOWN	2.51E-28	2.59E-28
novel_mir49	-1.29065831	DOWN	1.79E-15	1.58E-15
novel_mir567	-1.62350323	DOWN	1.93E-15	1.70E-15
ssc-miR-122	-1.488998972	DOWN	8.98E-86	1.30E-85
ssc-miR-129a-5p	-1.454395851	DOWN	3.62E-86	5.27E-86
ssc-miR-194b-5p	-1.057208557	DOWN	3.00E-38	3.51E-38
ssc-miR-199b-3p	-2.255474013	DOWN	0	0
ssc-miR-199b-5p	-1.218503253	DOWN	7.17E-12	5.52E-12
ssc-miR-206	-2.176211531	DOWN	0.000915313	0.000341273
ssc-miR-218-5p	-1.142424055	DOWN	1.04E-83	1.48E-83
ssc-miR-369	-1.878362355	DOWN	3.86E-14	3.26E-14
ssc-miR-411	-1.138076402	DOWN	2.03E-08	1.32E-08
ssc-miR-432-5p	-1.145689587	DOWN	5.04E-11	3.71E-11
ssc-miR-4332	-1.174186696	DOWN	1.14E-24	1.14E-24
ssc-miR-4334-3p	-1.07982083	DOWN	4.06E-39	4.78E-39
ssc-miR-451	-1.098656926	DOWN	8.88E-242	2.09E-241
ssc-miR-493-5p	-1.026107971	DOWN	0.002667718	0.000908341
ssc-miR-9-1	-2.746308682	DOWN	4.32E-97	6.54E-97
ssc-miR-9841-3p	-2.081149334	DOWN	1.37E-33	1.52E-33
novel_mir106	2.336379307	UP	1.16E-39	1.37E-39
novel_mir12	1.139769481	UP	0	0
novel_mir2	3.044520211	UP	0	0
novel_mir234	3.219194073	UP	9.44E-76	1.31E-75
novel_mir24	6.425946028	UP	0	0
novel_mir245	1.30670844	UP	2.44E-08	1.58E-08
novel_mir3	6.731975673	UP	0	0
novel_mir310	1.694605865	UP	3.33E-225	7.53E-225
novel_mir351	1.487831648	UP	3.31E-09	2.25E-09
novel_mir434	1.017042664	UP	1.54E-19	1.45E-19
novel_mir522	1.19262783	UP	1.62E-19	1.52E-19
novel_mir539	1.064241579	UP	8.39E-23	8.18E-23
novel_mir593	1.762387924	UP	1.65E-14	1.42E-14
novel_mir89	3.129864492	UP	5.39E-217	1.20E-216
ssc-miR-1277	1.096542321	UP	4.73E-21	4.56E-21
ssc-miR-1285	2.30004471	UP	1.34E-290	3.49E-290
ssc-miR-129b	2.639116549	UP	4.42E-96	6.63E-96
ssc-miR-151-3p	1.405595005	UP	0	0
ssc-miR-181d-5p	1.12718902	UP	0	0
ssc-miR-190a	1.269254058	UP	9.30E-52	1.19E-51
ssc-miR-218b	1.813324005	UP	0	0
ssc-miR-24-2-5p	1.140463424	UP	8.86E-48	1.11E-47
ssc-miR-24-3p	1.363494934	UP	0	0
ssc-miR-324	1.255654734	UP	1.61E-187	3.17E-187
ssc-miR-339-5p	1.243201213	UP	4.13E-162	7.73E-162
ssc-miR-383	1.66927852	UP	3.63E-05	1.72E-05
ssc-miR-542-5p	1.147380709	UP	6.74E-113	1.08E-112

(Continued)

TABLE 2 | Continued

miRNA id	log2Ratio (Sample/control)	Up/down regulation	P-value	Q-value
ssc-miR-545-3p	1.467644658	UP	2.62E-05	1.26E-05
ssc-miR-551a	1.743279101	UP	1.66E-11	1.26E-11
ssc-miR-671-5p	1.198396549	UP	0	0
ssc-miR-676-5p	1.610384831	UP	0.001821424	0.000649716
ssc-miR-874	1.565878137	UP	1.11E-159	2.05E-159
ssc-miR-885-5p	1.250986748	UP	2.49E-115	4.07E-115
ssc-miR-9-2	4.409446546	UP	6.45E-115	1.04E-114

with a NEB Next[®] Ultra[™] Directional RNA Library Prep Kit for Illumina[®] (NEB, USA). The constructed libraries were evaluated on an Agilent Bioanalyzer 2100 system (12). RNA integrity was checked by microcapillary electrophoresis using an Agilent 2100 Bioanalyzer with an RNA 6000 Nano chip kit (Agilent Technologies, Germany) (15). Sequencing was then performed using a paired-end 125-cycle rapid run on an Illumina HiSeq2500 (Illumina Inc., San Diego, CA, USA). Low-quality reads were removed, and the clean reads were filtered from the raw reads and mapped to the porcine reference genome (*Sus scrofa* v10.2). The mapped reads for each sample were independently assembled using Cufflinks (v2.1.1).

RNA-seq Data Analysis

The raw sequencing data (raw reads) were preserved in FASTQ format. Clean data of high quality were then aligned to the *Sus scrofa* genome assembly (*Sus Scrofa* v10.2) using TopHat2 (v2.0.9) (24). The transcriptome of each sample was assembled from the mapped reads using Cufflinks (v2.1.1) (25).

Initial Screening of miRNAs and RNAs

Significantly differentially regulated miRNAs and RNAs were screened in several steps. Firstly, the miRNAs and RNAs with no signals to the background were excluded in each group. Secondly, the differentially expressed miRNAs and RNAs were screened by a parametric t-test with a Benjamini-Hochberg adjusted significance level of 0.001. A usual selection criterion for biomarkers was set at an alpha level of 0.05 for Benjamini-Hochberg adjusted significance values. The relative expression levels of miRNAs were then normalized as the trimmed mean of M-values (TMM) using the edge R package. An absolute value of $\log_2 \text{FC} \geq 2$ and an $\text{FDR} < 0.01$ was considered as significantly differentially expressed compared with the control group.

Gene Expression Analysis

The transcriptome data have been deposited in the National Center for Biotechnology Information Gene Expression Omnibus (GEO, <https://www.ncbi.nlm.nih.gov/sra>) under the accession number SRP158168. Gene expression levels were estimated by fragments per kilobase per million (FPKM) values obtained using Cufflinks software. The discrepant genes were

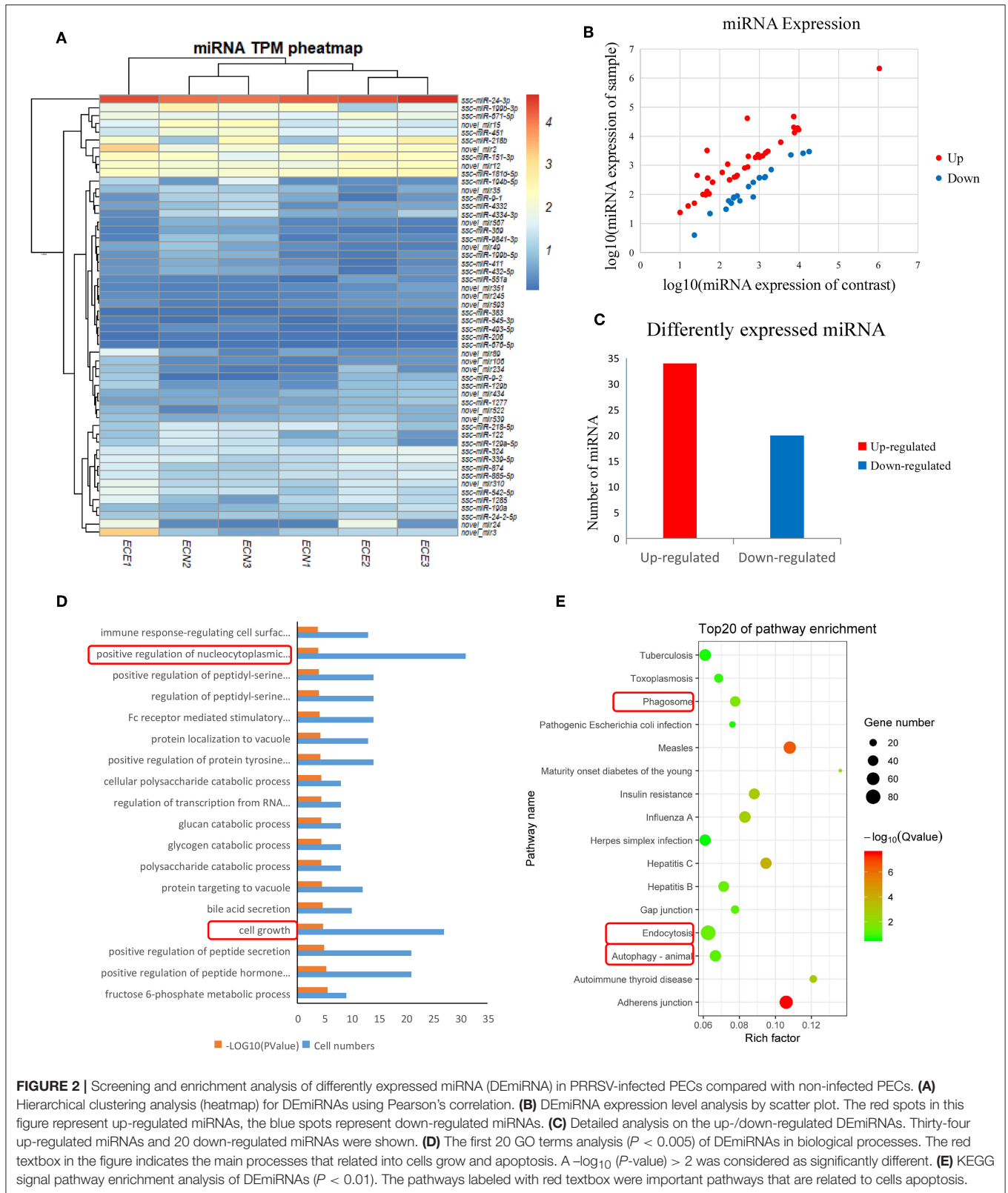


TABLE 3 | mRNA and lncRNA sequence counts between samples.

Sample	Total raw reads	Total clean reads	Total clean base	Clean reads ratio
ECE1	133380672	126897516	12689751600	95.14%
ECE2	133380286	126455060	12645506000	94.81%
ECE3	133377020	126587268	12658726800	94.91%
ECN1	133380108	126253656	12625365600	94.66%
ECN2	135026492	126770380	12677038000	93.89%
ECN3	135027010	127240652	12724065200	94.23%

analyzed only with an absolute value of \log_2 FC ≥ 2 and an FDR < 0.01 .

Prediction of the Function of lncRNAs

Prediction of the functions of lncRNAs was performed using their related *cis*- and *trans*-target mRNAs that were functionally well-annotated. Potentially *cis*-regulated target genes were deemed as 10 kb in genomic distance from the lncRNA and potentially *trans*-regulated target genes were identified using RNAplex software (26, 27).

GO (Gene Ontology) and KEGG Enrichment Analysis

DElncRNA, DEmiRNA, and DEGs were screened. GO and KEGG analyses of the differentially expressed genes (DEGs) were carried out with the GO seq R package (v1.18.0) (28) and KOBAS software (v2.0) (29).

Integrated Analysis of DEGs and DElncRNA Target Genes

Based on the competing endogenous RNA (ceRNA) hypothesis, we constructed DEGs and DElncRNAs crosstalk networks. The networks were constructed by integrating prior knowledge of miRNA and lncRNA interactions (30).

Real-Time PCR Analysis

Real-time PCR was performed using SYBR[®] Green PCR Master Mix (TaKaRa, Dalian, China) and an Applied Biosystems 7500 Real-Time PCR System. All primers used in this study are listed in Table 1.

RNA Interference and Western Blotting

The small interfering RNA to reduce the expression of *miR-339-5p* was synthesized (Table 1) and transfected into PECs. After PECs were infected PRRSV, apoptosis were analyzed as described above. Subsequently, the Caspase 3 and Caspase 8 protein were detected by Western blotting. After extracted protein by PIPA (Beyotime, Jiang Su, China), the protein were then checked by SDS-PAGE. After the protein were transferred into PVDF membrane. The Caspase 3 antibody (Cat: ab2302, Abcam) and Caspase 8 antibody (Cat: ab25901, Abcam) were incubated with the membrane separately. The membrane were exposed after incubated with Goat anti-rabbit antibody (Cat: ab6721, Abcam).

Statistical Analysis

DEG expression analysis results are presented as the mean \pm SEM and were analyzed by one-way ANOVA test. GO and KEGG analyses were assessed by Fisher's *t*-test. A $P < 0.05$ was considered as significantly different. All of the co-expressed relationships were predicted using Cytoscape ClueGO plug-in (v2.3.2, <http://apps.cytoscape.org/apps/cluego>) as a complementary analysis method. Only Benjamini–Hochberg-corrected values of $P < 0.05$ were considered statistically significant.

RESULTS

Isolation and Purification of PRRSV-Susceptible PECs

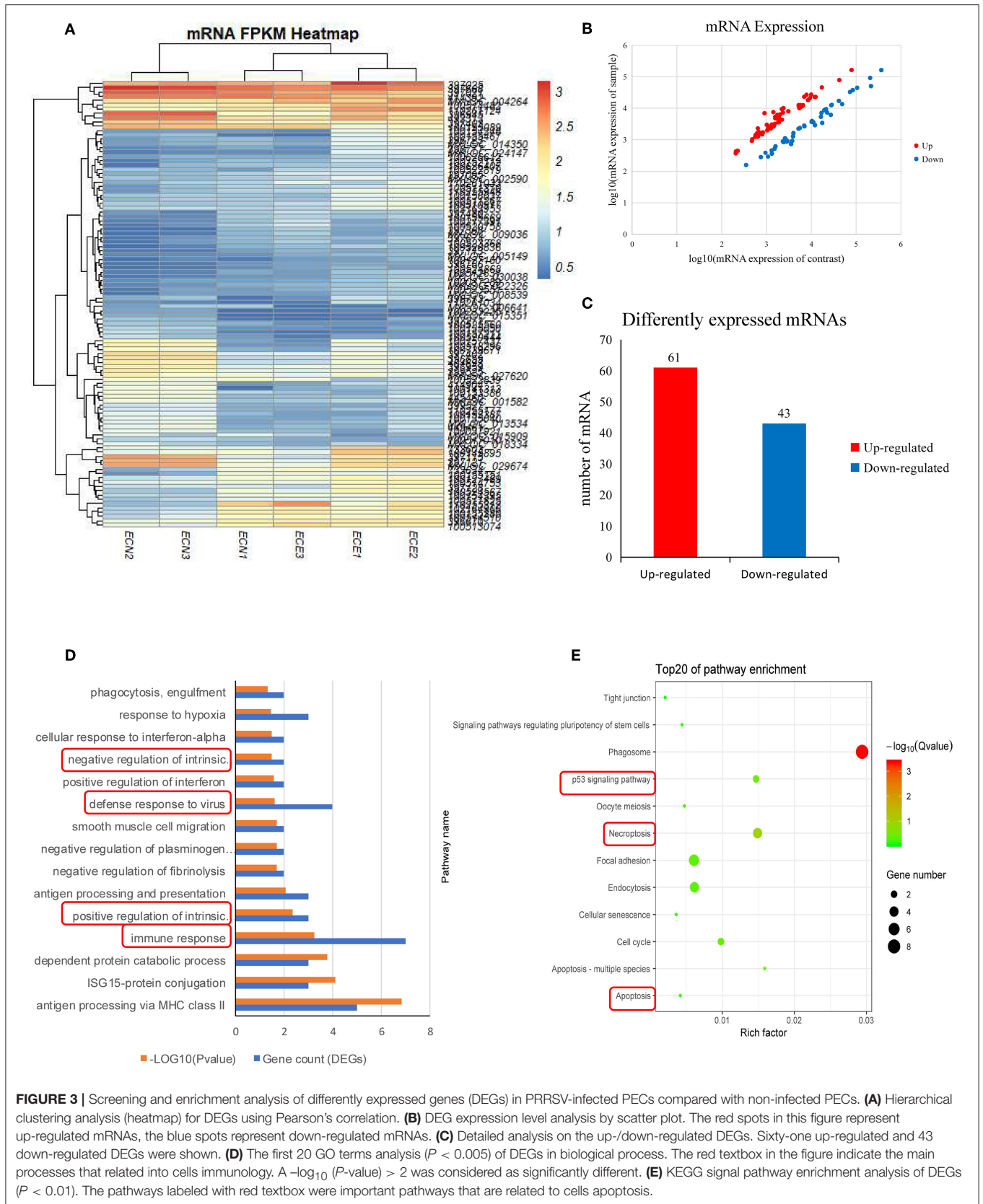
PECs were isolated, purified, and then dyed with Keratin-18 and Sialoadhesin antibodies, separately. The green fluorescence shown in Figure 1A indicated that the isolated cells were Keratin-18 and Sialoadhesin positive, suggesting a potential PRRSV infectivity of them. Subsequently, the PRRSV susceptibility of PECs was evaluated by assessing the apoptosis of PRRSV infected PECs. The rate of apoptosis caused by PRRSV was obviously increased, indicating that the cells isolated were susceptible to PRRSV (Figure 1B).

Landscape of the miRNA Transcriptomes in PECs

We generated six miRNA expression profiles of PECs from Large White pigs, three of each from mock- and PRRSV-infected PECs, respectively. Clean reads were obtained after filtering for reads with low quality and removing adaptor sequences from the raw reads (Supplemental Table 1). A total of 54 DEmiRNAs were obtained (Table 2) and a heatmap is shown in Figure 2A. miRNA expression levels are illustrated by scatter plot in Figure 2B. Detailed analysis of the up-/down-regulated DEmiRNAs is shown in Figure 2C. The observed up-regulation of specific DEmiRNAs might contribute to reproductive failure in pigs caused by PRRSV infection.

Functional Annotation of the Target Genes of Specific DEmiRNAs

DEmiRNAs were predicted by the validated miRNA-targets database (mirTarBase 4.5) and 1,453 targets were captured (Supplemental Table 2). Subsequently, the target genes were analyzed by GO and KEGG analyses. Figure 2D shows the first 20 GO terms ($P < 0.005$) from a biological process analysis (Supplemental Table 3). The GO analysis showed that the target genes were significantly enriched in cell growth ($P = 0.0000186$) and positive regulation of nucleocytoplasmic transport ($P = 0.00018$). KEGG analysis of DEmiRNAs suggested that cytophagy (phagosome and endocytosis pathways) and autophagy were the main pathways influencing cell apoptosis (Figure 2E).



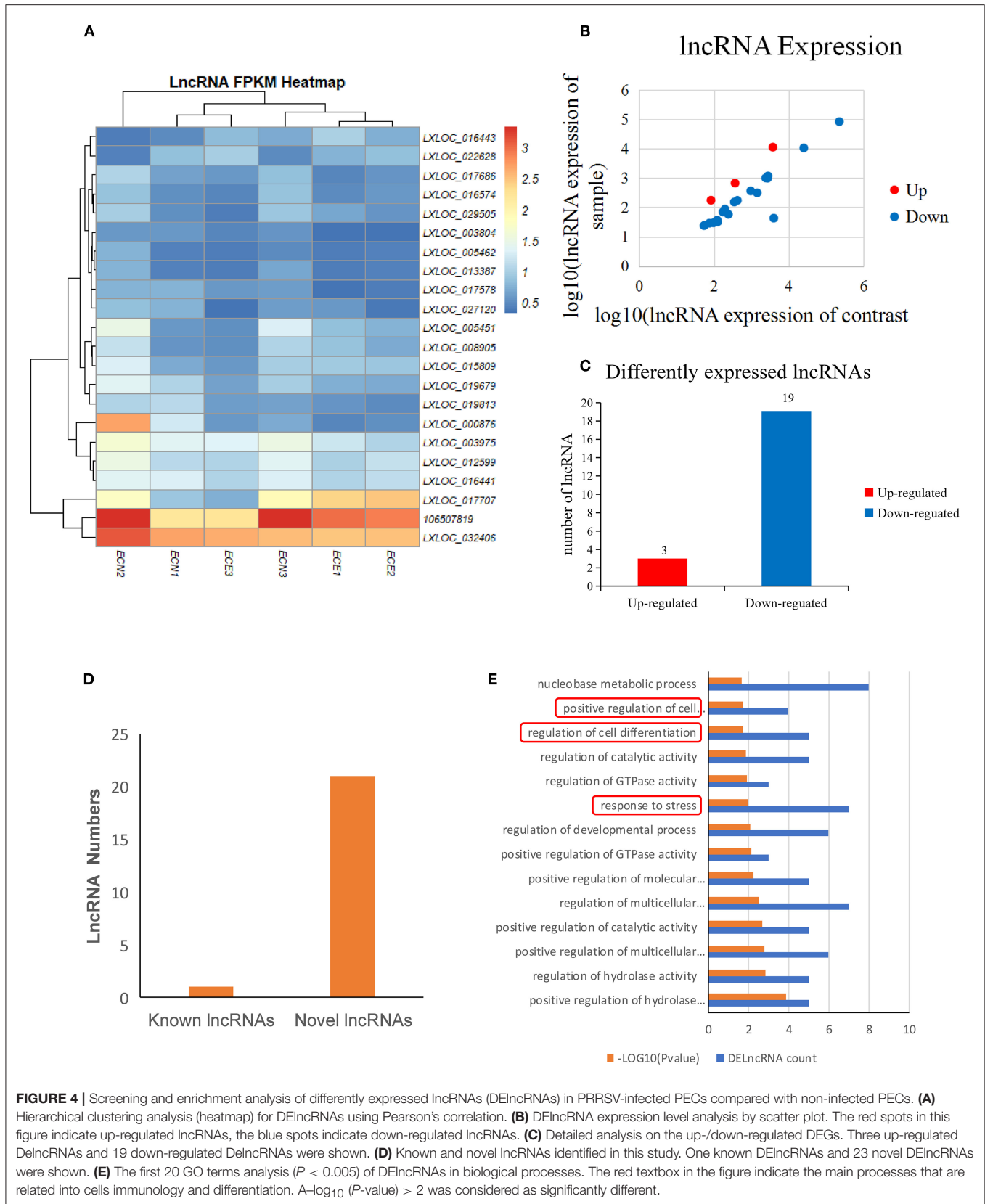


TABLE 4 | Differentially expressed lncRNAs.

GeneID	Length	Contrast readnum	Sample readnum	log2Ratio	Up/down regulation	P value	Q value
LXLOC_000876	237	196	88	-1.017573944	Down	1.07E-08	8.45E-09
LXLOC_005451	243	55.88	24.86	-1.030801443	Down	0.002027419	0.000811493
LXLOC_019679	251	54	24	-1.03222072	Down	0.002387418	0.000935437
LXLOC_019813	229	349.04	153.07	-1.051496539	Down	4.51E-15	5.10E-15
LXLOC_017686	2165.79	2768.54	1187.19	-1.08387024	Down	2.08E-113	1.37E-112
LXLOC_027120	352	25173	10710.43	-1.095156477	Down	0	0
LXLOC_016574	599	2415.04	1012.51	-1.116406646	Down	6.04E-104	3.63E-103
106507819	243	421.94	174.17	-1.138837433	Down	3.73E-20	5.14E-20
LXLOC_029505	460	173.29	70.22	-1.165530221	Down	1.93E-09	1.60E-09
LXLOC_017578	234	74.95	29.08	-1.228196927	Down	3.86E-05	2.09E-05
LXLOC_013387	1201	960	368	-1.245624358	Down	3.67E-50	1.10E-49
LXLOC_012599	1114	223984	84141	-1.274810528	Down	0	0
LXLOC_003975	3473	2707	996	-1.304772959	Down	3.16E-148	2.70E-147
LXLOC_032406	252	96	30	-1.540367624	Down	3.13E-08	2.38E-08
LXLOC_008905	238	121	37	-1.57170559	Down	2.88E-10	2.53E-10
LXLOC_016441	215	124.84	32.43	-1.806975052	Down	1.56E-12	1.57E-12
LXLOC_003804	234	242.7	58.27	-1.920644611	Down	9.47E-25	1.52E-24
LXLOC_005462	674	1428	316	-2.038295234	Down	5.45E-148	4.66E-147
LXLOC_015809	262	3960.58	43.36	-6.37549887	Down	0	0
LXLOC_022628	621	3760	11364	1.733370451	Up	0	0
LXLOC_016443	336	83	176	1.222096469	Up	4.43E-11	4.10E-11
LXLOC_017707	874	366.61	675.19	1.01875168	Up	7.68E-29	1.40E-28

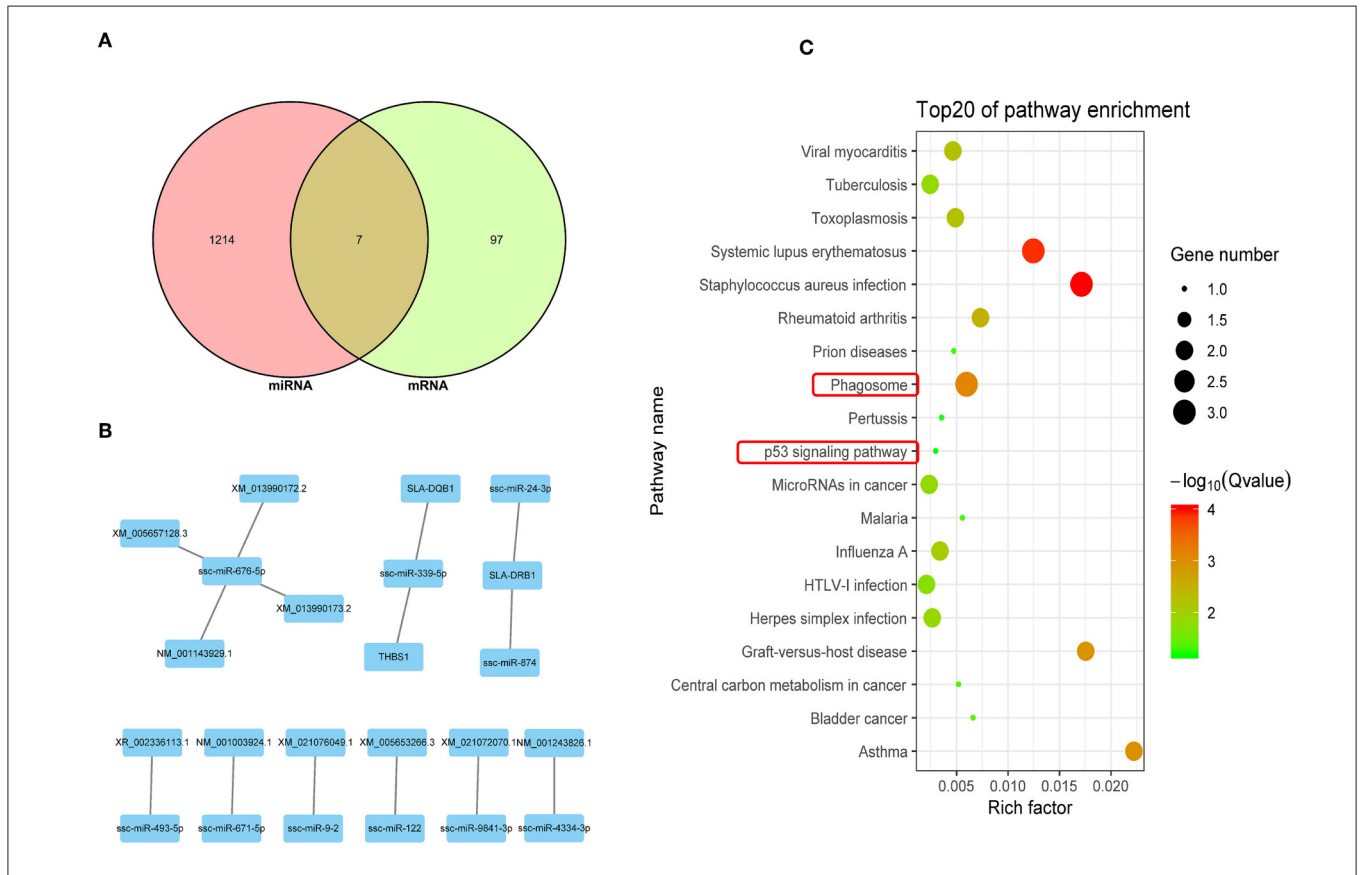


FIGURE 5 | Integrated analysis of DEGs and DEmiRNA target genes. **(A)** Venn map analysis of DEmiRNA target genes and DEGs. Seven co-expressed genes from the DEGs and DEmiRNA target genes were shown. **(B)** Regulatory relationship between DEGs and DEmiRNAs. Nine DEmiRNAs that are related to the DEGs regulatory were shown. **(C)** KEGG analysis based on reciprocal DEmiRNAs and DEGs ($P < 0.05$). The phagosome and p53 signal are the main pathway that are related to cells apoptosis.

TABLE 5 | Differentially expressed miRNAs and corresponding differentially expressed genes.

miRNA	Gene name	Fold change
ssc-miR-339-5p	CD1D	-3.184223813
	SLA-DQB1	-1.549162701
	THBS1	-1.020771929
	SLC3A1	-1.019117703
ssc-miR-324	SLC3A1	-1.019117703
	CAPN3	-3.66965064
	OLFML2B	-4.562735437
	FGL2	-1.704504473
ssc-miR-383	FGL2	-1.704504473
	PALM2	-1.627830465
	HAPLN1	-3.219847723
	ITM2A	-4.385857674
ssc-miR-874	DRD1	-1.263025381
	DRD1	-1.263025381
	SLC2A4	-1.210219022
	CD79A	-4.03222072
ssc-miR-24-3p	SLA-DRB1	-1.888055067
	SLA-DRB1	-1.888055067
	SLC2A4	-1.210219022
	VSIG4	-1.089529403
	MPEG1	-2.658762324
ssc-miR-181d-5p	SIGIRR	-7.057840178
	RLN2	-2.658762324
	ZFP37	-1.199910451
	SELP	-4.562735437
	LOC100517161	-1.325340399

Summary of RNA-Seq in PECs

Six mRNA expression profiles of PECs were generated from Large White pigs after filtering for reads with low quality and removing adaptor sequences (Table 3), three of each from mock- and PRRSV-infected PECs, respectively. Clean reads were then assembled and 104 DEGs were detected ($FC > 2$ and $FDR < 0.01$) (Supplemental Table 4). A heatmap of the DEGs was then constructed and is shown in Figure 3A. mRNA expression levels are displayed in a scatter plot in Figure 3B. Detailed analysis of the up-/down-regulated DEGs is shown in Figure 3C. The identified up-regulated mRNAs may play important roles in PEC damage caused by PRRSV.

Enrichment of DEGs

DEGs were then assessed by GO and KEGG pathway analysis. Immune response ($P = 0.000593$), defense response to virus ($P = 0.0232515$), and intrinsic apoptotic signaling pathways (positive, $P = 0.004421637$; negative, $P = 0.03125$) were revealed in the GO analysis (Figure 3D; Supplemental Table 5). Three potential pathways were predicted (p53 signal pathway, necroptosis, and apoptosis; $P < 0.05$), and were mainly involved in cell survival (Figure 3E).

Summary of lncRNA Sequencing in PECs

The expression of lncRNAs was then evaluated and a heatmap of the DElncRNAs was created based on the expression levels (Figure 4A; Table 4). A total of 22 DElncRNA genes and 24 potential transcripts were predicted and exhibited obvious changes in the scatter plot ($P < 0.05$) (Figure 4B; Supplemental Table 6). Detailed analysis on the up-/down-regulated DElncRNAs suggested that the down-regulated lncRNAs may play important roles in PRRSV infection processing (Figure 4C). The analysis also revealed that the known lncRNAs represent only a small portion of all DElncRNAs (Figure 4D).

Enrichment of DElncRNA Target Genes

DElncRNA isoforms were then evaluated and 109 isoforms were detected (Supplemental Table 7). GO term analysis of the DElncRNAs hinted that they were mainly involved cell differentiation ($P = 0.018$) and response to stress ($P = 0.01$) (Figure 4E; Supplemental Table 8) in PRRSV infected PECs.

Integrated Analysis of DEGs and DEmiRNA Target Genes

An integrated analysis of DEGs and DEmiRNA target genes was carried out to screen for co-expressed genes. The Venn diagram in Figure 5A shows 7 co-expressed genes from the DEGs and DEmiRNA target genes. The relationships between the DEGs and DEmiRNAs were then evaluated and the correlations are shown in Figure 5B ($P < 0.05$) and listed in Table 5. KEGG analysis suggested that the phagosome and p53 signal pathways play important roles during PRRSV infection in PECs ($P < 0.01$) (Figure 5C).

Integrated Analysis of DEGs and DElncRNA Target Genes

The Venn diagram shown in Figure 6A illustrates 3 potential genes co-expressed among the DEGs and DElncRNA target genes. DEGs and DElncRNA crosstalk networks were then evaluated and are shown in Figure 6B and listed in Table 6, based on the 10 potential genes regulated by lncRNAs ($P < 0.05$). The phagosome and p53 signal pathways identified in the KEGG pathway analysis suggested that PRRSV could cause cell apoptosis in PECs ($P < 0.01$) (Figure 6C).

Genes Related to PRRSV-Induced Apoptosis in PECs

Related DEGs and DEmiRNAs that were identified in the crosstalk network analysis were verified by real-time PCR. *miR-339-5p* and *miR-181-5p* were found to be significantly up-regulated in PRRSV-infected PECs compared to the control (Figure 7). Additionally, the target genes of *miR-339-5p* and *miR-181-5p* were evaluated and the expression of *SLC3A1*, *THBS1*, *SLA-DQB1*, *ZFP37*, and *LOC100517161* were found to be down-regulated compared to the control group (Figure 7).

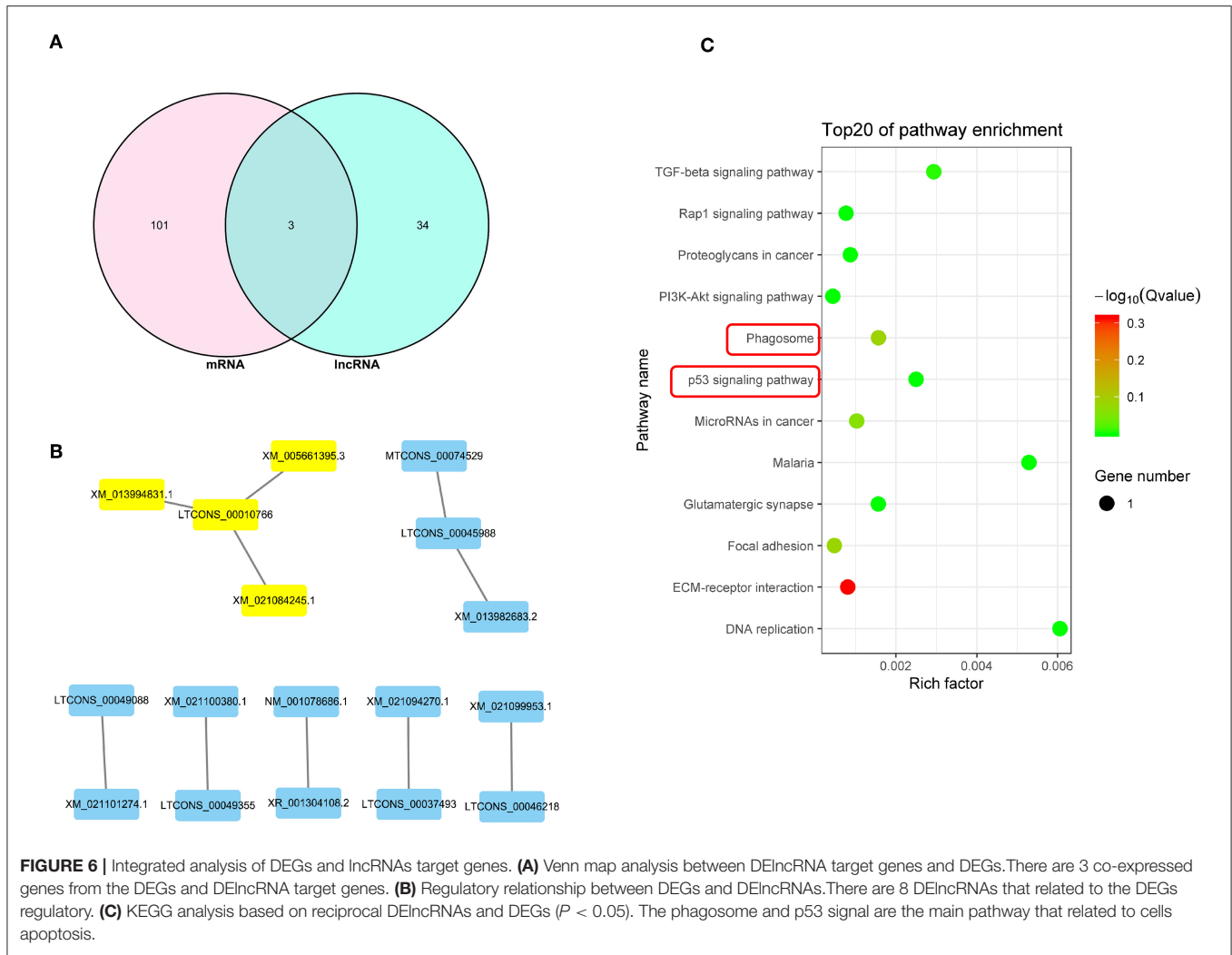


FIGURE 6 | Integrated analysis of DEGs and lncRNAs target genes. **(A)** Venn map analysis between DElncRNA target genes and DEGs. There are 3 co-expressed genes from the DEGs and DElncRNA target genes. **(B)** Regulatory relationship between DEGs and DElncRNAs. There are 8 DElncRNAs that related to the DEGs regulatory. **(C)** KEGG analysis based on reciprocal DElncRNAs and DEGs ($P < 0.05$). The phagosome and p53 signal are the main pathway that related to cells apoptosis.

TABLE 6 | Correlation analysis between differentially expressed mRNAs and lncRNAs.

GeneID	mRNA log2Ratio	Annotation	Regulation	P-value	lncRNA geneID	lncRNA log2Ratio	Regulation	P-value	Pearson correlation	Spearman correlation
XM_013994831.1	1.2301	MUM1X7	Up	3.73E-25	LTCONS_000107866	-1.0322	Down	2.39E-03	-0.7028	-0.7714
XM_021084245.1	-7.047	MUM1X12	Down	2.12E-17	LTCONS_000107866	-1.0322	Down	2.39E-03	0.6607	0.6761
XM_005661395.3	5.9011	GAMT	Up	2.77E-08	LTCONS_000107866	-1.0322	Down	2.39E-03	-0.9902	-0.8804
XM_021094270.1	-2.3265	ANKRD27X3	Down	2.37E-72	LTCONS_00037493	-1.1655	Down	1.93E-09	0.8015	0.8857
MTCONS_00074529	-6.1824		Down	1.46E-10	LTCONS_00045988	-1.0515	Down	4.51E-15	0.6741	0.6761
XM_013982683.2	1.9422	FBXO16	Up	2.18E-10	LTCONS_00045988	-1.0515	Down	4.51E-15	-0.7887	-0.6667
XM_021099953.1	-7.0377	RGS6	Down	6.85E-45	LTCONS_00046218	-1.3048	Down	3.16E-148	0.9844	0.8804
XM_021101274.1	-1.8287	ZFP493	Down	3.87E-23	LTCONS_00049088	-1.2282	Down	3.86E-05	0.8703	0.759
XM_021100380.1	-1.3566	ANKRD17	Down	1.03E-95	LTCONS_00049355	-1.5717	Down	2.88E-10	0.6131	0.8286
NM_001078686.1	-1.2773	ODAM	Down	1.93E-03	XR_001304108.2	-1.2748	Down	0.00E+00	0.9484	0.9276

Functional Analysis of miR-339-5p

The effect of *miR-339-5p* knock down on the apoptosis of PECs was analyzed. Cells transfected with *miR-339-5p* inhibitor (antisense oligonucleotides) obviously increased its survival

ratio compared with the normal PECs upon PRRSV infection (Figure 8A). Western blotting also indicated that *miR-339-5p* could reduce the level of expressed cleavage Caspase 3 rather than Caspase 8 protein (Figure 8B).

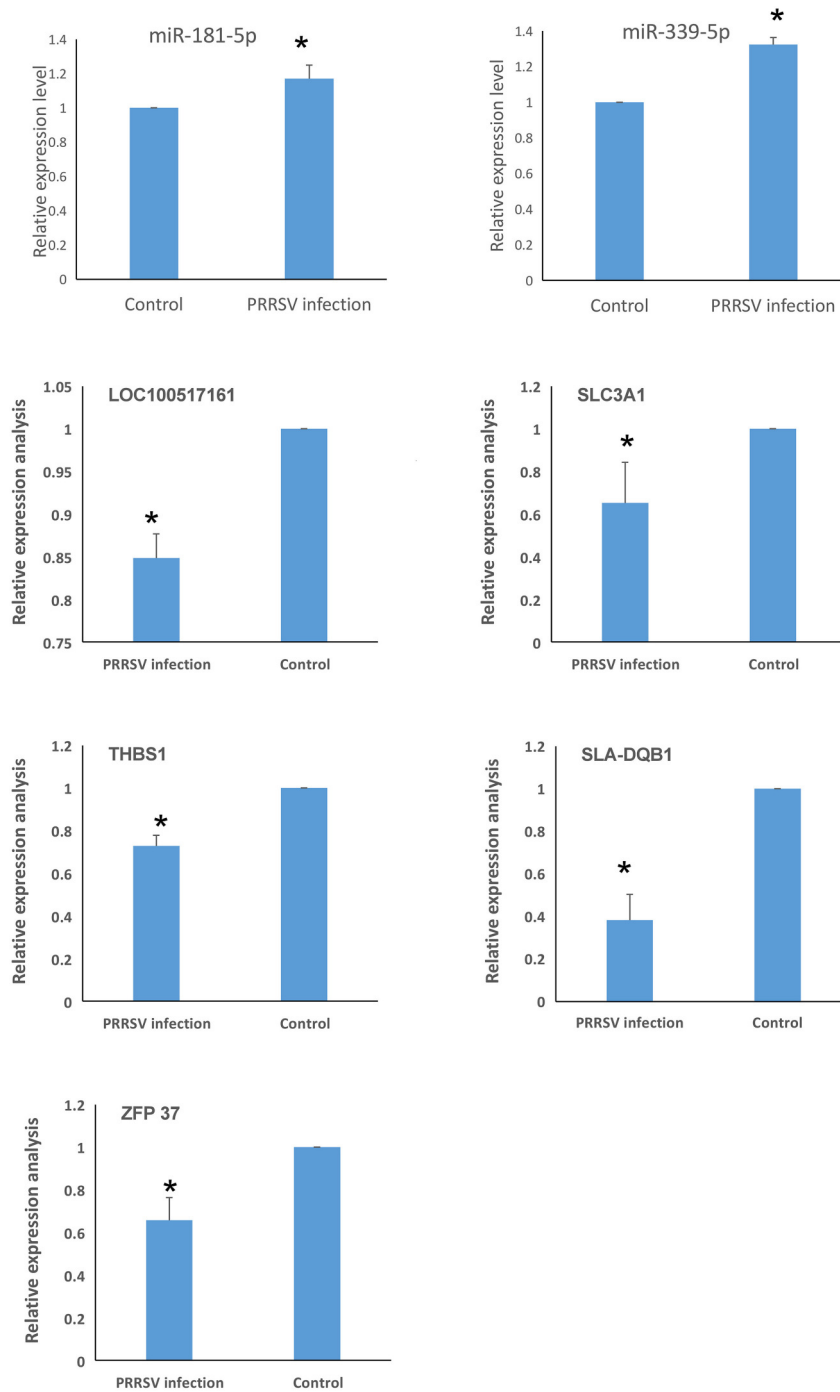
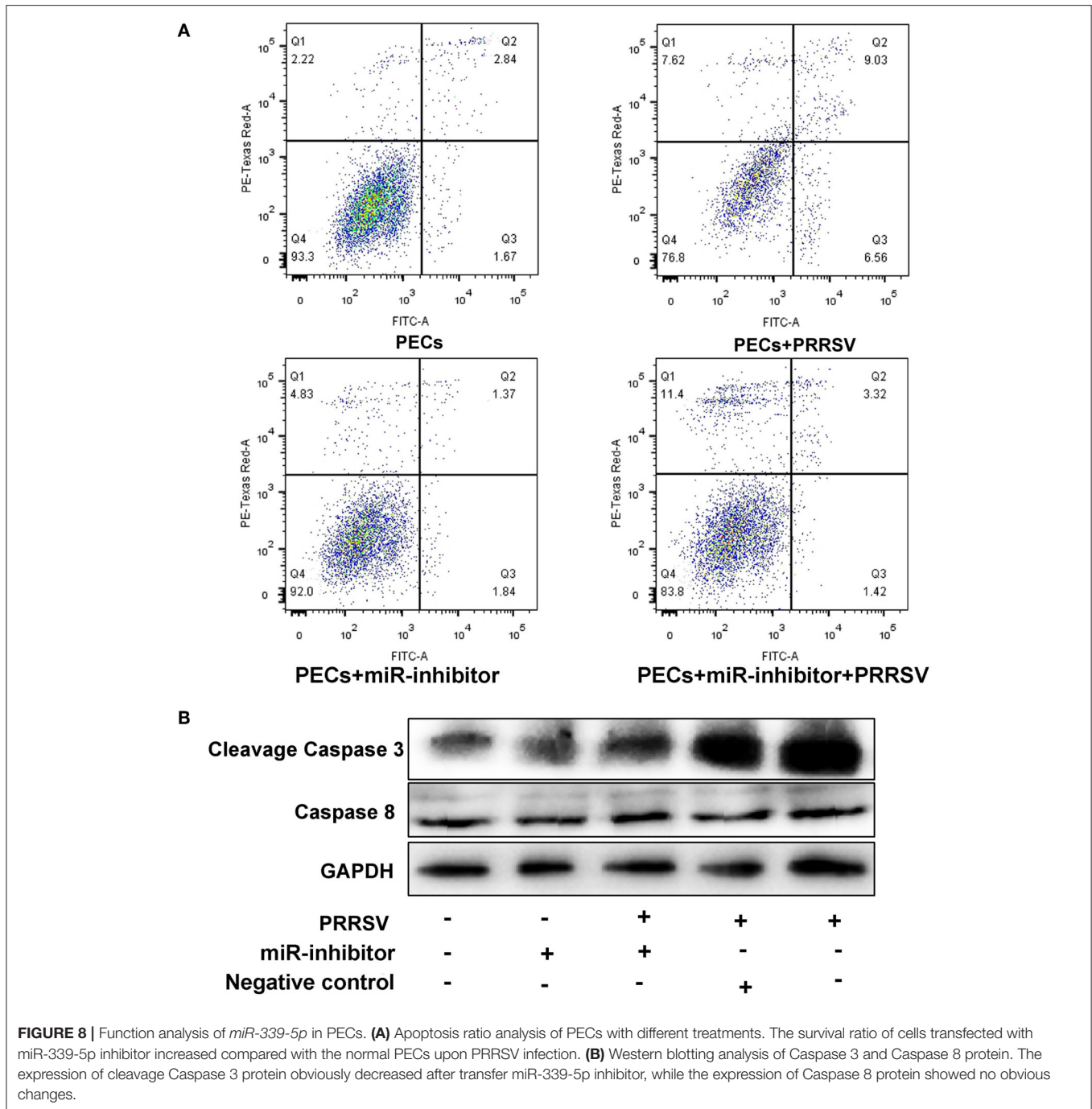


FIGURE 7 | Identification of genes related to PRRSV-induced apoptosis in PECs ($*P < 0.05$). *miR-339-5p* and *miR-181-5p* were significantly up-regulated in PRRSV-infected PECs compared to control cells. The expression of *SLC3A1*, *THBS1*, *SLA-DQB1*, *ZFP37*, and *LOC100517161* were down-regulated in PRRSV-infected PECs compared to non-infected PECs ($P < 0.05$).

DISCUSSION

In this study, we identified a link between apoptosis of placental cells and PECs and reproductive failure in pregnant sows. We

first isolated Sn-positive PECs and examined apoptosis rates by flow cytometry. Apoptosis rates were significantly higher in PRRSV-infected cells than in control cells. Subsequently, the whole PEC transcriptome was analyzed for DEGs and GO/KEGG



pathways. Differentially expressed miRNA, mRNA and lncRNA were identified in PRRSV-infected PECs. Integration analysis identified differentially co-expressed target genes and regulatory crosstalk networks. Regulatory crosstalk networks of miRNAs with DEGs and lncRNAs with DEGs were constructed separately. Pathway enrichment revealed that the phagosome and p53 pathways were likely the main signals resulting in cell apoptosis in PECs.

Placental cells and PECs are the main target cells of PRRSV invasion (6). PRRSV could infect CD163- and Sn-positive macrophages in the late period of pregnancy, ultimately resulting in PEC apoptosis (6). Feng et al. isolated and generated a PEC line susceptible to PRRSV (4). The isolated cells in this study expressed CK-18 and Sn protein, which verified the cell type as previously reported (4). A cell apoptosis test confirmed the susceptibility of PECs and verified

that PEC apoptosis was caused by PRRSV, as in previous reports (3, 31, 32).

Several studies have focused on miRNA profile variation in PRRSV-infected target cells. Xu et al. analyzed PRRSV-infected PAM cells at different infection time points and screened clusters of miRNAs (33). Li et al. compared miRNA profiles in different pig breeds and obtained 6 DEmiRNAs that may contribute to Landrace-specific responses of PRRSV infection (34). miRNA profile changes were also investigated by Zhou et al. in Marc-145 cells (35). Significant differences exist between our study and others. One difference is that our study mainly focused on the reproductive system (PECs), while others have primarily concentrated on the respiratory system (lung samples, PAM cells, etc.) (32–35). The miRNAs identified in this study are different from those in previous reports. Another difference is that the DEmiRNA enrichment analysis showed enrichment for cell growth, autophagy, and phagosome pathways, which differs from previous reports (35).

mRNA profiles were also investigated in many previous studies, and several tissues and cells were found to be prone to damage caused by PRRSV, such as peripheral blood mononuclear cells (15), lung dendritic cells (36), Marc-145 cells (37), and lung tissues (34). Discrepancies among the differentially expressed mRNAs identified in previous studies may be due to differences in pig breeds and PRRSV strain. In this study, mRNA transcription profiles were created and the data identified 104 DEGs that were mainly enriched in cell apoptosis and the p53 signal pathway. The signal pathways identified in this study are the same as reported previously (5).

The only published research related to lncRNA profile changes was carried out by Zhang et al. in PAM cells (12). They identified 299 DELncRNAs, which were mainly enriched in viral infection and immune response. Their data also suggested that lncRNAs might play regulatory roles in virus–host interactions. Significant differences were found in our study compared with Zhang et al. in PAM cells (12). PAM cells are mononuclear cells sensitive to PRRSV, but the cells used in this study were epithelial cells, which mainly play defensive roles during viral infection. Moreover, Zhang's study mainly focused on the immune system (12), which is different from this study.

Integrated analysis of DEmiRNAs and DEG profiles was carried out to find common genes with altered expression. There were 6 DEmiRNAs and 7 DEGs found in this study. A regulatory network was built based on the correlation between these DEmiRNAs and DEGs. The identified miRNAs (*ssc-miR-339-5p* and *ssc-miR-181d-5p*) and genes (*SLA-DQB1*, *THBS1*, *SLC3A1*, *ZFP37*, and *LOC100517161*) were screened after analysis of genes related to the phagosome and p53 signal pathways. Previous studies reported up-regulation of *miR-339-5p* could activate the p53 apoptosis pathway via targeting *MDM2* mRNA in tumor cells; in contrast, down-regulated *miR-339-5p* increased cell proliferation (38–41). *miR-181* has been widely investigated and is known to be a key gene influencing gene expression and cell apoptosis, especially in PRRSV-infected cells (42–46). *miR-181d* acts as a tumor suppressor by targeting *K-ras* and *Bcl-2* (47). *SLA-DQB1* has been recognized as an antigen presentation gene (48, 49). *THBS1* participates in the p53 signal pathway and was

found to influence the survival of tumor cells in a previous study (50). Expression of *SLC3A1* enhanced tumorigenesis in tumor cells, whereas inhibition of *SLC3A1* suppressed tumor growth (51).

Analysis of DEG and DELncRNA profiles revealed a correlation between mRNA and lncRNA, and also suggested that the p53 signal pathway is the main pathway that influences PEC apoptosis. The genes that were involved in the p53 signal pathway were then evaluated and compared with previous studies. *LTCONS_00010766* and *LTCONS_00045988* have never been reported in previous studies, but the target genes of these lncRNAs (*MUMIX12*, *MUMIX7*, *GAMT*, and *FBXO16*) are known as key genes influencing the p53 pathway (52–56). Functional analysis of *miR-339-5p* exhibited that the *miR-339-5p* gene is involved into p53 pathway, which is as same as previous studies (38–40).

CONCLUSIONS

In summary, we first isolated Sn-positive PECs and then checked apoptosis rates by flow cytometry. Apoptosis rates in PRRSV-infected PECs were significantly higher than in control cells. Whole PEC transcriptome analysis revealed a total of 54 DEmiRNAs, 104 DEGs, 22 DELncRNAs, and 109 isoforms that are mainly involved in apoptosis, necroptosis, and the p53 signal pathway. Integration analysis of DEmiRNA and DEG profiles identified two lncRNAs and five genes that may participate in apoptosis. Integration analysis of DEGs and DELncRNAs profiles showed that target genes by *LTCONS_00010766* and *LTCONS_00045988* were related to the apoptosis signal pathway. Pathway enrichment revealed that the phagosome and the p53 pathways are likely the main signals contributing to cell apoptosis in PECs.

ETHICS STATEMENT

All sows used in this study were housed in livestock housing and fed *ad libitum*. The sacrifice of sows was carried out with sodium barbital after anesthesia. All procedures involving animals were approved by the Animal Care and Use Committee of Shandong Agricultural University.

AUTHOR CONTRIBUTIONS

FS, LG, and YJ designed the experiments and drafted the manuscript. KZ, SD, and YL carried out animal care, prepared samples, and performed the experiments. DW and CM performed the data processing and biological information analysis. FS, YW, CZ, and YJ conceived the study and the experimental design, and helped draft the manuscript. All authors have read and approved the final manuscript.

FUNDING

This research was financially supported by grants from the Agricultural Breed Project of Shandong Province

(2016), funds from the Shandong Double Tops Program (no.SYL2017YSTD12), funds from the National Key Technology R&D Program (2015BAD03B02-8), and funds from the Postdoctoral Program in Shandong Agricultural University.

REFERENCES

- Wang G, Yu Y, Tu Y, Tong J, Liu Y, Zhang C, et al. Highly pathogenic porcine reproductive and respiratory syndrome virus infection induced apoptosis and autophagy in thymic of infected piglets. *PLoS ONE*. (2015) 10:e0128292. doi: 10.1371/journal.pone.0128292
- Li S, Zhou A, Wang J, Zhang S. Interplay of autophagy and apoptosis during PRRSV infection of Marc145 cell. *Infect Genet Evol*. (2016) 39:51–4. doi: 10.1016/j.meegid.2016.01.011
- Karniyuchuk UU, Nauwynck HJ. Pathogenesis and prevention of placental and transplacental porcine reproductive and respiratory syndrome virus infection. *Vet Res*. (2013) 44:95. doi: 10.1186/1297-9716-44-95
- Feng L, Zhang X, Xia X, Li Y, He S, Sun H. Generation and characterization of a porcine endometrial endothelial cell line susceptible to porcine reproductive and respiratory syndrome virus. *Virus Res*. (2013) 171:209. doi: 10.1016/j.virusres.2012.11.015
- Ao Z, Li S, Khan FA, Zhang S. Autophagy postpones apoptotic cell death in PRRSV infection through Bad-Beclin1 interaction. *Virulence*. (2016) 7:98–109. doi: 10.1080/21505594.2015.1131381
- Novakovic P, Harding JC, Aldissi AN, Detmer SE. Type 2 porcine reproductive and respiratory syndrome virus infection increases apoptosis at the maternal-fetal interface in late gestation pregnant gilts. *PLoS ONE*. (2017) 12:e0173360. doi: 10.1371/journal.pone.0173360
- Harding JC, Ladinig A, Novakovic P, Detmer SE, Wilkinson JM, Yang T, et al. Novel insights into host responses and reproductive pathophysiology of porcine reproductive and respiratory syndrome caused by PRRSV-2. *Vet Microbiol*. (2017) 209:114. doi: 10.1016/j.vetmic.2017.02.019
- Lee SM, Kleiboeker SB. Porcine reproductive and respiratory syndrome virus induces apoptosis through a mitochondria-mediated pathway. *Virology*. (2007) 365:419–34. doi: 10.1016/j.virol.2007.04.001
- Karniyuchuk UU, Saha D, Vanhee M, Geldhof M, Cornillie P, Caij AB, et al. Impact of a novel inactivated PRRS virus vaccine on virus replication and virus-induced pathology in fetal implantation sites and fetuses upon challenge. *Theriogenology*. (2012) 78:1527–37. doi: 10.1016/j.theriogenology.2012.06.015
- Huo Y, Fan L, Yin S, Dong Y, Guo X, Yang H, et al. Involvement of unfolded protein response, p53 and Akt in modulation of porcine reproductive and respiratory syndrome virus-mediated JNK activation. *Virology*. (2013) 444:233–40. doi: 10.1016/j.virol.2013.06.015
- Cong P, Xiao S, Chen Y, Wang L, Gao J, Li M, et al. Integrated miRNA and mRNA transcriptomes of porcine alveolar macrophages (PAM cells) identifies strain-specific miRNA molecular signatures associated with H-PRRSV and N-PRRSV infection. *Mol Biol Rep*. (2014) 41:5863–75. doi: 10.1007/s11033-014-3460-7
- Zhang J, Sun P, Gan L, Bai W, Wang Z, Li D, et al. Genome-wide analysis of long noncoding RNA profiling in PRRSV-infected PAM cells by RNA sequencing. *Sci Rep*. (2017) 7:4952. doi: 10.1038/s41598-017-05279-z
- Xiao SQ, Jia JY, Mo DL, Wang QW, Qin LM, He ZY, et al. Understanding PRRSV infection in porcine lung based on genome-wide transcriptome response identified by deep sequencing. *PLoS ONE*. (2010) 5:e11377. doi: 10.1371/journal.pone.0011377
- Zhou P, Zhai S, Zhou X, Lin P, Jiang T, Hu X, et al. Molecular characterization of transcriptome-wide interactions between highly pathogenic porcine reproductive and respiratory syndrome virus and porcine alveolar macrophages *in vivo*. *Int J Biol Sci*. (2012) 8:947. doi: 10.7150/ijbs.8.124
- Islam MA, Großebrinkhaus C, Pröll MJ, Uddin MJ, Rony SA, Tesfaye D, et al. Deciphering transcriptome profiles of peripheral blood mononuclear cells in response to PRRSV vaccination in pigs. *BMC Genomics*. (2016) 17:641. doi: 10.1186/s12864-016-2849-1
- Islam MA, Großebrinkhaus C, Pröll MJ, Uddin MJ, Aqter SR, Tesfaye D, et al. PBMC transcriptome profiles identifies potential candidate genes and functional networks controlling the innate and the adaptive immune response to PRRSV vaccine in Pietrain pig. *PLoS ONE*. (2017) 12:e0171828. doi: 10.1371/journal.pone.0171828
- Islam MA, Neuhoﬀ C, Rony SA, Große-Brinkhaus C, Uddin MJ, Hölker M, et al. MT170 Integrated network analysis for mRNAs and miRNAs expressed in PRRSV vaccinated peripheral blood mononuclear cells of pigs. In: *Conference*. Dublin (2017).
- Xiong Y, Fang JH, Yun JB, Yang J, Zhang Y, Jia WH, et al. Effects of microRNA-29 on apoptosis, tumorigenicity, and prognosis of hepatocellular carcinoma. *Hepatology*. (2010) 51:836–45. doi: 10.1002/hep.23380
- Wang Y, Lee CGL. MicroRNA and cancer-focus on apoptosis. *J Cell Mol Med*. (2009) 13:12–23. doi: 10.1111/j.1582-4934.2008.00510.x
- Deng D, Wang L, Chen Y, Li B, Xue L, Shao N, et al. MicroRNA-124-3p regulates cell proliferation, invasion, apoptosis, and bioenergetics by targeting PIM1 in astrocytoma. *Cancer Sci*. (2016) 107:899. doi: 10.1111/cas.12946
- Cui Z, Ren S, Lu J, Wang F, Xu W, Sun Y, et al. The prostate cancer-up-regulated long noncoding RNA PlncRNA-1 modulates apoptosis and proliferation through reciprocal regulation of androgen receptor. *Urol Oncol*. (2013) 31:1117–23. doi: 10.1016/j.urolonc.2011.11.030
- Zhang Z, Zhu Z, Watabe K, Zhang X, Bai C, Xu M, et al. Cell death and differentiation - negative regulation of lncRNA GAS5 by miR-21. *Cell Death Different*. (2013) 20:1558–68. doi: 10.1038/cdd.2013.110
- Wei ZY, Wang XB, Zhang HY, Yang CH, Wang YB, Xu DH, et al. Inhibitory effects of indigowoad root polysaccharides on porcine reproductive and respiratory syndrome virus replication *in vitro*. *Antiviral Ther*. (2011) 16:357–63. doi: 10.3851/IMP1755
- Kim D, Pertea G, Trapnell C, Pimentel H, Kelley R, Salzberg SL. TopHat2: accurate alignment of transcriptomes in the presence of insertions, deletions and gene fusions. *Genome Biol*. (2013) 14:R36. doi: 10.1186/gb-2013-14-4-r36
- Trapnell C, Williams BA, Pertea G, Mortazavi A, Kwan G, Baren MJV, et al. Transcript assembly and quantification by RNA-Seq reveals unannotated transcripts and isoform switching during cell differentiation. *Nat Biotechnol*. (2010) 28:511–5. doi: 10.1038/nbt.1621
- Tafer H, Hofacker IL. RNAplex: a fast tool for RNA-RNA interaction search. *Bioinformatics*. (2008) 24:2657–63. doi: 10.1093/bioinformatics/btn193
- Zeng N, Cong W, Liu S, Qi M, Lei Z, Ge X, et al. Transcriptome analysis reveals dynamic gene expression profiles in porcine alveolar macrophages in response to the chinese highly pathogenic porcine reproductive and respiratory syndrome virus. *BioMed Res Int*. (2018) 2018:1–23. doi: 10.1155/2018/1538127
- Young MD, Wakefield MJ, Smyth GK, Alicia O. Gene ontology analysis for RNA-seq: accounting for selection bias. *Genome Biol*. (2010) 11:R14. doi: 10.1186/gb-2010-11-2-r14
- Mao X, Cai T, Olyarchuk JG, Wei L. Automated genome annotation and pathway identification using the KEGG Orthology (KO) as a controlled vocabulary. *Bioinformatics*. (2005) 21:3787–93. doi: 10.1093/bioinformatics/bti430
- Shuang Y, Ning Q, Zhang G, Hong S, Zhen W, Li Y. Construction of differential mRNA-lncRNA crosstalk networks based on ceRNA hypothesis uncover key roles of lncRNAs implicated in esophageal squamous cell carcinoma. *Oncotarget*. (2016) 7:85728–40. doi: 10.18632/oncotarget.13828

SUPPLEMENTARY MATERIAL

The Supplementary Material for this article can be found online at: <https://www.frontiersin.org/articles/10.3389/fimmu.2019.01221/full#supplementary-material>

31. Mocarski ES, Upton JW, Kaiser WJ. Viral infection and the evolution of caspase 8-regulated apoptotic and necrotic death pathways. *Nat Rev Immunol.* (2011) 12:79. doi: 10.1038/nri3131
32. Karniychuk UU, Saha D, Geldhof M, Vanhee M, Cornillie P, Broeck WVD, et al. Porcine reproductive and respiratory syndrome virus (PRRSV) causes apoptosis during its replication in fetal implantation sites. *Microbial Pathog.* (2011) 51:194–202. doi: 10.1016/j.micpath.2011.04.001
33. Xu D. Genome-Wide miRNA expression profiling of pietrain PAM infected with/without PRRSV. *Plant Anim Genome.* (2014) 9:79. Available online at: <https://pag.confex.com/pag/xxii/webprogram/Paper12030.html>
34. Li J, Chen Z, Zhao J, Fang L, Fang R, Xiao J, et al. Difference in microRNA expression and editing profile of lung tissues from different pig breeds related to immune responses to HP-PRRSV. *Sci. Rep.* (2015) 5:9549. doi: 10.1038/srep09549
35. Zhou A, Li S, Zhang S. miRNAs and genes expression in MARC-145 cell in response to PRRSV infection. *Infect Genet Evol.* (2014) 27:173–80. doi: 10.1016/j.meegid.2014.07.023
36. Pröll MJ, Neuhoﬀ C, Schellander K. Transcriptome profile of lung dendritic cells after *in vitro* porcine reproductive and respiratory syndrome virus (PRRSV) infection. *PLoS ONE.* (2017) 12:e0187735. doi: 10.1371/journal.pone.0187735
37. Wei Y, Li J, Zhang Y, Xue C, Cao Y. Tandem 3' UTR patterns and gene expression profiles of marc-145 cells during PRRSV infection. *Virol Sinica.* (2018) 33:335–44. doi: 10.1007/s12250-018-0045-y
38. Zhang C, Liu J, Wang X, Wu R, Lin M, Laddha SV, et al. MicroRNA-339-5p inhibits colorectal tumorigenesis through regulation of the MDM2/p53 signaling. *Oncotarget.* (2014) 5:9106–17. doi: 10.18632/oncotarget.2379
39. Wu Z, Wu Q, Wang C, Wang X, Wang Y, Zhao J, et al. MiR-339-5p inhibits breast cancer cell migration and invasion *in vitro* and may be a potential biomarker for breast cancer prognosis. *BMC Cancer.* (2010) 10:542. doi: 10.1186/1471-2407-10-542
40. Li Y, Zhang X, Yang Z, Li Y, Han B, Chen LA. miR-339-5p inhibits cell migration and invasion *in vitro* and may be associated with the tumor-node-metastasis staging and lymph node metastasis of non-small cell lung cancer. *Oncol Lett.* (2014) 8:719–25. doi: 10.3892/ol.2014.2165
41. Jansson MD, Damas ND, Lees M, Jacobsen A, Lund AH. miR-339-5p regulates the p53 tumor-suppressor pathway by targeting MDM2. *Oncogene.* (2015) 34:1908–18. doi: 10.1038/onc.2014.130
42. Li D, Jian W, Wei C, Song H, Gu Y, Luo Y, et al. Down-regulation of miR-181b promotes apoptosis by targeting CYLD in thyroid papillary cancer. *Int J Clin Exp Pathol.* (2014) 7:7672–80.
43. Wang Y, Zhou H, Liu X, Han Y, Pan S. MiR-181a inhibits human trabecular meshwork cell apoptosis induced by H₂O₂ through the suppression of NF- κ B and JNK pathways. *Adv Clin Exp Med.* (2018) 27:577–82. doi: 10.17219/acem/69135
44. Xue-kun G, Qiong Z, Li G, Ning L, Xin-xin C, Wen-hai F. Increasing expression of microRNA 181 inhibits porcine reproductive and respiratory syndrome virus replication and has implications for controlling virus infection. *J Virol.* (2013) 87:1159. doi: 10.1128/JVI.02386-12
45. Lv X, Mao Z, Lyu Z, Zhang P, Zhan A, Wang J, et al. miR181c promotes apoptosis and suppresses proliferation of metanephric mesenchyme cells by targeting Six2 *in vitro*. *Cell Biochem Funct.* (2015) 32:571–9. doi: 10.1002/cbf.3052
46. Qin Y, Zhao JY, Luo WT, Li J, Liu J and Zhang JS. Mechanism research of miR-181 regulating human lens epithelial cell apoptosis. *Int Eye Sci.* (2015) 15:759–63. doi: 10.3980/j.issn.1672-5123.2015.5.04
47. Wang XF, Shi ZM, Wang XR, Cao L, Wang YY, Zhang JX, et al. MiR-181d acts as a tumor suppressor in glioma by targeting K-ras and Bcl-2. *J Cancer Res Clin Oncol.* (2012) 138:573–84. doi: 10.1007/s00432-011-1114-x
48. Liu ZZ, Xia JH, Xin LL, Wang ZG, Qian L, Wu SG, et al. Swine leukocyte antigen class II genes (SLA-DRA, SLA-DRB1, SLA-DQA, SLA-DQB1) polymorphism and genotyping in Guizhou minipigs. *Genet Mol Res.* (2015) 14:15256–66. doi: 10.4238/2015.November.30.1
49. Le M, Choi H, Choi MK, Cho H, Kim JH, Seo HG, et al. Development of a simultaneous high resolution typing method for three SLA class II genes, SLA-DQA, SLA-DQB1, and SLA-DRB1 and the analysis of SLA class II haplotypes. *Gene.* (2015) 564:228–32. doi: 10.1016/j.gene.2015.03.049
50. Lawler J, Miao WM, Duquette M, Bouck N, Bronson RT, Hynes RO. Thrombospondin-1 gene expression affects survival and tumor spectrum of p53-deficient mice. *Am J Pathol.* (2001) 159:1949–56. doi: 10.1016/S0002-9440(10)63042-8
51. Jiang Y, Cao Y, Wang Y, Li W, Liu X, Lv Y, et al. Cysteine transporter SLC3A1 promotes breast cancer tumorigenesis. *Theranostics.* (2017) 7:1036–46. doi: 10.7150/thno.18005
52. Gualco G, Weiss LM, Bacchi CE. MUM1/IRF4: A review. *Appl Immunohistochem Mol Morphol.* (2010) 18:301–10. doi: 10.1097/PAI.0b013e3181cf1126
53. Wasco MJ, Fullen D, Su L, Ma L. The expression of MUM1 in cutaneous T-cell lymphoproliferative disorders. *Hum Pathol.* (2008) 39:557–63. doi: 10.1016/j.humpath.2007.08.013
54. Ide T, Brownendres L, Chu K, Ongusaha PP, Ohtsuka T, Eldeiry WS, et al. GAMT, a p53-inducible modulator of apoptosis, is critical for the adaptive response to nutrient stress. *Mol Cell.* (2013) 51:552. doi: 10.1016/j.molcel.2013.08.005
55. Ide T, Chu K, Aaronson SA, Lee SW. GAMT joins the p53 network: branching into metabolism. *Cell Cycle.* (2010) 9:1706–10. doi: 10.4161/cc.9.9.11473
56. Liu Y, Lear T, Iannone O, Shiva S, Corey C, Rajbhandari S, et al. The Proapoptotic F-box Protein Fbxl7 regulates mitochondrial function by mediating the ubiquitylation and proteasomal degradation of survivin. *J Biol Chem.* (2015) 290:11843–52. doi: 10.1074/jbc.M114.629931

Conflict of Interest Statement: The authors declare that the research was conducted in the absence of any commercial or financial relationships that could be construed as a potential conflict of interest.

Copyright © 2019 Zhang, Ge, Dong, Liu, Wang, Zhou, Ma, Wang, Su and Jiang. This is an open-access article distributed under the terms of the Creative Commons Attribution License (CC BY). The use, distribution or reproduction in other forums is permitted, provided the original author(s) and the copyright owner(s) are credited and that the original publication in this journal is cited, in accordance with accepted academic practice. No use, distribution or reproduction is permitted which does not comply with these terms.